model of a SN Ia explosion is incomplete. The most natural solution to this problem that would make the results consistent with observations would be to assume that the turbulent flame triggers a detonation. A thermonuclear detonation wave could propagate through the WD with velocities $\sim 10^9$ cm/s (*49*, *50*) and would quickly burn all the material near the center, leaving only the low-density outer layers unburned. For a density below 5×10^7 g/cm^3, a detonation would produce intermediate-mass elements (*25*) that are observed in spectra of SNe Ia. A detonation would also partially smooth out composition inhomogeneities that are predicted by the deflagration model and that may be incompatible with observations (*51*). Remaining asymmetries may account for a weak polarization recently detected in SN Ia spectra (*52*, *53*).

One-dimensional (*25*, *28*–*32*) and 2D (*26*, *27*) delayed-detonation models were the most successful in explaining observable characteristics of SNe Ia. These models, however, use the time for detonation initiation as a free parameter because the DDT problem is intrinsically 3D and still unsolved. A large-scale 3D model also cannot reproduce DDT phenomena that involve physical processes occurring on small unresolved scales. One approach to solving this problem is to study in much more detail the types of reacting flows created by 3D deflagrations and to look for situations that create the right types of "hot spots" that we know (*54*) are the sources of detonation initiation.

References and Notes

1. J. C. Wheeler, R. P. Harkness, *Rep. Prog. Phys.* **53**, 1467 (1990).
2. A. V. Filippenko, *Annu. Rev. Astron. Astrophys.* **35**, 309 (1997).
3. J. C. Wheeler, *Am. J. Phys.*, in press.
4. S. E. Woosley, T. A. Weaver, *Annu. Rev. Astron. Astrophys.* **24**, 205 (1986).
5. D. Branch, A. M. Khokhlov, *Phys. Rep.* **256**, 53 (1995).
6. J. C. Wheeler, R. P. Harkness, A. M. Khokhlov, P. A. Höflich, *Phys. Rep.* **256**, 211 (1995).
7. K. Nomoto, K. Iwamoto, N. Kishimoto, *Science* **276**, 1378 (1997).
8. D. Branch, *Annu. Rev. Astron. Astrophys.* **36**, 17 (1998).
9. W. Hillebrandt, J. C. Niemeyer, *Annu. Rev. Astron. Astrophys.* **38**, 191 (2000).
10. A. Burrows, *Nature* **403**, 727 (2000).
11. F. Hoyle, W. A. Fowler, *Astrophys. J.* **132**, 565 (1960).
12. M. M. Phillips, *Astrophys. J.* **413**, L105 (1993).
13. M. Hamuy *et al.*, *Astron. J.* **109**, 1 (1995).
14. A. G. Riess, W. H. Press, R. P. Kirshner, *Astrophys. J.* **438**, L17 (1995).
15. S. Perlmutter *et al.*, *Nature* **391**, 51 (1998).
16. S. Perlmutter *et al.*, *Astrophys. J.* **517**, 565 (1999).
17. B. P. Schmidt *et al.*, *Astrophys. J.* **507**, 46 (1998).
18. A. G. Riess *et al.*, *Astron. J.* **116**, 1009 (1998).
19. A. G. Riess *et al.*, *Astrophys. J.* **560**, 49 (2001).
20. P. A. Höflich *et al.*, *Astrophys. J.* **472**, L81 (1996).
21. W. D. Arnett, *Astrophys. Space Sci.* **5**, 180 (1969).
22. C. J. Hansen, J. C. Wheeler, *Astrophys. Space Sci.* **3**, 464 (1969).
23. K. Nomoto, D. Sugimoto, S. Neo, *Astrophys. Space Sci.* **39**, L37 (1976).
24. _____, F.-K. Thielemann, K. Yokoi, *Astrophys. J.* **286**, 644 (1984).
25. A. M. Khokhlov, *Astron. Astrophys.* **245**, 114 (1991).
26. D. Arnett, E. Livne, *Astrophys. J.* **427**, 315 (1994).
27. _____, *Astrophys. J.* **427**, 330 (1994).
28. H. Yamaoka, K. Nomoto, T. Shigeyama, F.-K. Thielemann, *Astrophys. J.* **393**, L55 (1992).
29. A. M. Khokhlov, E. Müller, P. A. Höflich, *Astron. Astrophys.* **270**, 223 (1993).
30. P. A. Höflich, *Astrophys. J.* **443**, 89 (1995).
31. _____, A. M. Khokhlov, J. C. Wheeler, *Astrophys. J.* **444**, 831 (1995).
32. _____, A. M. Khokhlov, *Astrophys. J.* **457**, 500 (1996).
33. A. M. Khokhlov, available online at http://arxiv.org/abs/astro-ph/0008463.
34. M. Reinecke, W. Hillebrandt, J. C. Niemeyer, *Astron. Astrophys.* **386**, 936 (2002).
35. _____, *Astron. Astrophys.* **391**, 1167 (2002).
36. Materials and Methods are available as supporting material on *Science* Online.
37. A. M. Khokhlov, *Astrophys. J.* **449**, 695 (1995).
38. _____, *J. Comput. Phys.* **143**, 519 (1998).
39. F. X. Timmes, S. E. Woosley, *Astrophys. J.* **396**, 649 (1992).
40. A. M. Khokhlov, E. S. Oran, J. C. Wheeler, *Astrophys. J.* **478**, 678 (1997).
41. _____, *Combust. Flame* **105**, 28 (1996).
42. P. A. Höflich, J. Stein, *Astrophys. J.* **568**, 779 (2002).
43. E. Livne, *Astrophys. J.* **406**, L17 (1993).
44. A. M. Khokhlov, *Astrophys. J.* **424**, L115 (1994).
45. D. J. Jeffery *et al.*, *Astrophys. J.* **397**, 304 (1992).
46. A. Fisher, D. Branch, P. Nugent, E. Baron, *Astrophys. J.* **481**, L89 (1997).
47. P. A. Mazzali, *Mon. Not. R. Astron. Soc.* **321**, 341 (2001).
48. R. P. Kirshner *et al.*, *Astrophys. J.* **415**, 589 (1993).
49. A. M. Khokhlov, *Mon. Not. R. Astron. Soc.* **239**, 785 (1989).
50. V. N. Gamezo, J. C. Wheeler, A. M. Khokhlov, E. S. Oran, *Astrophys. J.* **512**, 827 (1999).
51. R. C. Thomas, D. Kasen, D. Branch, E. Baron, *Astrophys. J.* **567**, 1037 (2002).
52. L. Wang, J. C. Wheeler, P. A. Höflich, *Astrophys. J.* **476**, L27 (1997).
53. D. A. Howell, P. A. Höflich, L. Wang, J. C. Wheeler, *Astrophys. J.* **556**, 302 (2001).
54. A. M. Khokhlov, E. S. Oran, *Combust. Flame* **119**, 400 (1999).

55. This work was supported in part by the NASA Astrophysics Theory program (NRA-99-01-ATP-130) and by the Naval Research Laboratory through the Office of Naval Research. Computing facilities were provided by the Department of Defense High Performance Computing Modernization Program. We would like to thank D. Branch, P. A. Höflich, E. Livne, M. Reinecke, L. Wang, and J. C. Wheeler for helpful discussions and the referees for useful comments.

Supporting Online Material

www.sciencemag.org/cgi/content/full/1078129/DC1
Materials and Methods
Figs. S1 and S2
Table S1
Movies S1 and S2

5 September 2002; accepted 22 October 2002
Published online 22 November 2002;
10.1126/science.1078129
Include this information when citing this paper.

Neuronal Activity in the Lateral Intraparietal Area and Spatial Attention

James W. Bisley* and Michael E. Goldberg

Although the parietal cortex has been implicated in the neural processes underlying visual attention, the nature of its contribution is not well understood. We tracked attention in the monkey and correlated the activity of neurons in the lateral intraparietal area (LIP) with the monkey's attentional performance. The ensemble activity in LIP across the entire visual field describes the spatial and temporal dynamics of a monkey's attention. Activity subtending a single location in the visual field describes the attentional priority at that area but does not predict that the monkey will actually attend to or make an eye movement to that location.

Visual attention, the ability to select a portion of the visual world for further processing, is necessary for the perception of the world around us (*1*). A number of studies have suggested that the lateral intraparietal area (LIP) of the posterior parietal cortex is involved in the generation of visual attention (*2*–*6*), on the basis of the well-established phenomenon of attentional enhancement of visual responses: A stimulus that is behaviorally important usually evokes an enhanced response relative to when that stimulus is unimportant. The enhanced response has traditionally been interpreted as reflecting attention to the stimulus itself, but some exceptions bring this interpretation into question. For example, in a cued visual reaction time task, the parietal response to a validly cued stimulus is often less than that to an invalidly cued stimulus (*3*, *7*). Furthermore, the probability of perceiving a stimulus at threshold

Laboratory of Sensorimotor Research, National Eye Institute, Bethesda, MD 20892, USA; Department of Neurology, Georgetown University School of Medicine, Washington, DC 20007, USA; Mahoney Center for Mind and Brain, Keck Center for Cognition and Plasticity, Center for Neurobiology and Behavior, Departments of Neurology and Psychiatry, Columbia University College of Physicians and Surgeons, and the New York State Psychiatric Institute, New York, NY 10032, USA.

*To whom correspondence should be addressed at Mahoney Keck Center for Mind and Brain, Center for Neurobiology and Behavior, New York State Psychiatric Institute, Unit 87, Room 5-06, 1051 Riverside Drive, New York, NY 10032, USA. E-mail: jwb2003@columbia.edu

depends not on the properties of the stimulus itself but rather on the subject's visual attention when the stimulus appears (*8*, *9*). To understand the relation of parietal activity to attention, we correlated the responses of neurons in LIP of monkeys with performance on a new task designed to measure both the spatial and temporal aspects of attention.

Measuring attention in the monkey. Three methods have been used to describe the locus of attention: a post hoc method (*10*); a reaction time method (*11*–*13*); and a contrast sensitivity method, which defines the spatial locus of attention as that area of the visual field with enhanced visual sensitivity (*14*–*18*). We used the latter because it allowed us to examine how attention changed over time and under different visual conditions (*19*).

Our task (fig. S1) had two components: the monkeys had to plan a saccade (rapid eye movement) to a remembered location and later had to decide whether to make the movement on the basis of a GO/NOGO stimulus (the probe). We varied the contrast of the probe and used each monkey's response to determine its contrast threshold. An animal's performance was better when the probe appeared at the location where the target had appeared (the saccade goal) than when it appeared elsewhere (Fig. 1A). This improved performance at the saccade goal was significant throughout the task [$P < 0.05$ by paired t test (Fig. 1B)]. We suggest that this lowering of the threshold is an index of the attention allocated to the goal of the planned saccade (*17*, *18*, *20*, *21*), and that the higher thresholds for the probe at other locations (*22*) represent the monkey's performance at loci to which attention has not been allocated a priori. We believe this difference is due to a true enhancement in sensitivity at the saccade goal and not to an increase in task difficulty caused by the spatial separation of the saccade target and the probe. The latter would have caused an upward rather than the observed leftward shift in the psychometric function (*23*).

A flashed object (*8*, *9*, *24*, *25*) or a pop-out stimulus (*26*) can attract attention, so we introduced a flashed, task-irrelevant distractor during the delay. The distractor was flashed on half of the trials and was presented either at the saccade goal or opposite the saccade goal (fig. S1B). The distractor was identical to the target in size, brightness, and duration, but appeared 500 ms after the target. When the distractor appeared in the opposite location to the target and the probe appeared 200 ms later, the perceptual threshold went down to the attentionally advantaged level at the site of the distractor (Fig. 1, C and D, red points) and rose to the baseline level at the saccade goal (Fig. 1, C and D, blue points). However, 700 ms after the distractor had appeared, performance was once again enhanced at the saccade goal and not at the distractor location, as was the case 1200 ms after the distractor appeared in monkey I, with a trend toward that result in monkey B. Thus, as in humans, a monkey's attention is involuntarily drawn to a flashed distractor. This occurs even when the animal is planning a saccade elsewhere, but the attentional effect of the distractor lasts for less than 700 ms, by which time attention has returned to the saccade goal. An important feature is the consistency of the attended performance. We found that whenever attention is placed at a location, whether driven there by the upcoming saccade (endogenous attention) or by the flashed distractor (exogenous attention), the

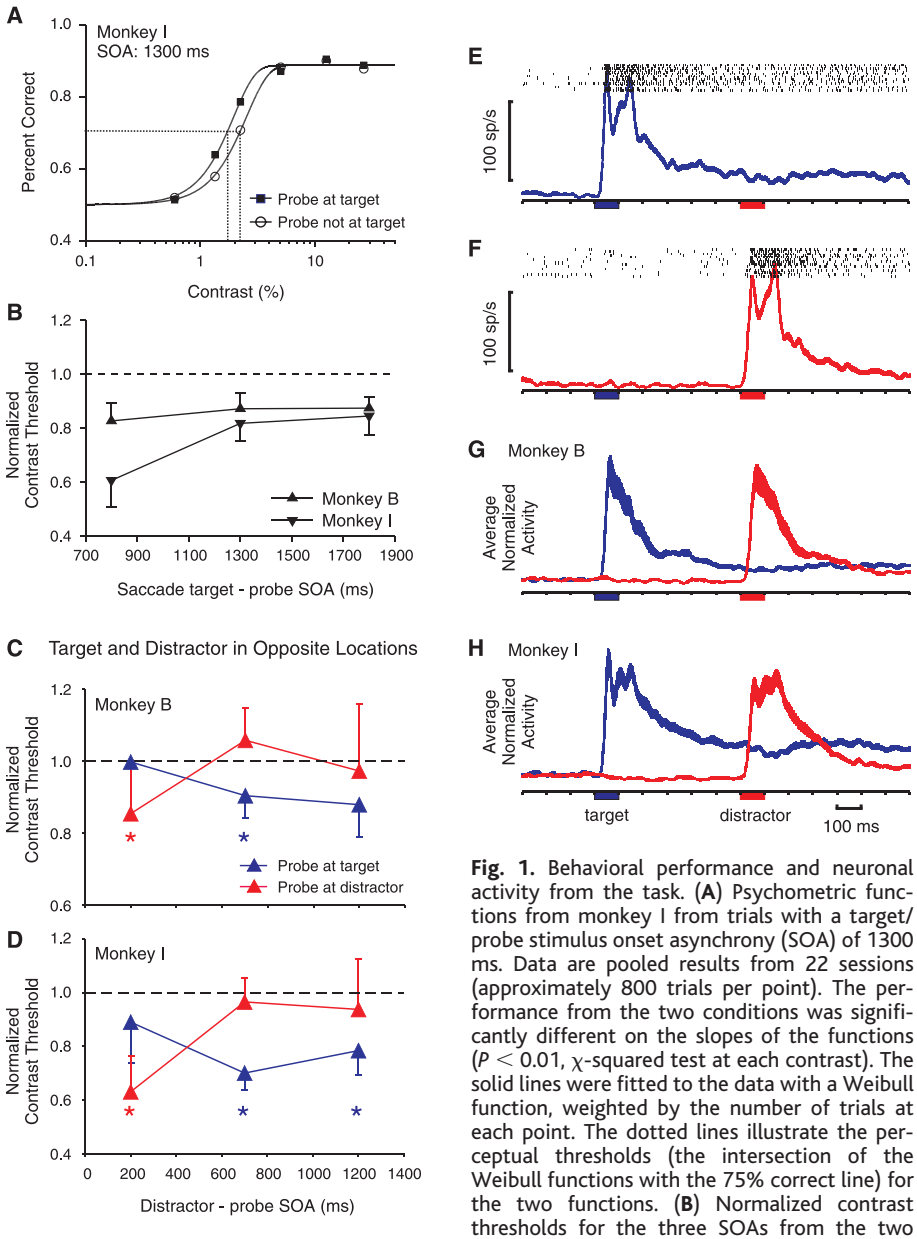

Fig. 1. Behavioral performance and neuronal activity from the task. (**A**) Psychometric functions from monkey I from trials with a target/probe stimulus onset asynchrony (SOA) of 1300 ms. Data are pooled results from 22 sessions (approximately 800 trials per point). The performance from the two conditions was significantly different on the slopes of the functions ($P < 0.01$, χ-squared test at each contrast). The solid lines were fitted to the data with a Weibull function, weighted by the number of trials at each point. The dotted lines illustrate the perceptual thresholds (the intersection of the Weibull functions with the 75% correct line) for the two functions. (**B**) Normalized contrast thresholds for the three SOAs from the two monkeys when the probe was at the location of the saccade goal. Data for each delay were normalized by the performance at that delay when the probe was not at the saccade goal (illustrated by the dashed line). Points significantly beneath the dashed line show attentional enhancement, and all points were significantly beneath the line (paired t test on prenormalized data). (**C** and **D**) Normalized contrast thresholds from trials in which the distractor appeared away from the saccade goal. Points significantly beneath the dashed line show attentional enhancement (asterisk indicates $P < 0.05$, paired t test on prenormalized data). (**E** to **H**) Responses of LIP neurons to the target appearing in the receptive field and the distractor appearing outside of the receptive field (blue traces) and to the distractor appearing in the receptive field after the target had appeared outside of the receptive field (red traces). Trace thickness represents the SEM, and the solid blue and red bars show the time and duration of the target and distractor, respectively. (E and F) Raster plots spike density functions from a single cell in LIP were recorded while the monkey was performing the task on threshold. (G) Averaged normalized spike density functions from 18 cells from monkey B. (H) Averaged normalized spike density functions from 23 cells from monkey I.

attentional advantage produced a similar benefit in performance.

Neuronal responses in LIP during the task. We hypothesized that activity in LIP would correlate with the placement of attention. We recorded the activity of 41 neurons in LIP with peripheral receptive fields in two hemispheres of the two monkeys from whom we gathered the psychophysical data. The neurons all had at least visual activity or both visual and memory activity. Figure 1, E and F, shows the response of a single neuron during the trials in which the target appeared in the receptive field of the neuron while the distractor flashed elsewhere (blue trace) and during the trials in which the distractor was presented in the receptive field and the target elsewhere (red trace). There was no difference between the responses for the saccade plan and the distractor measured at threshold or suprathreshold probe contrasts (supporting online text).

We normalized the responses of all the neurons by the mean value of all the points from each trial type for each cell and then calculated the average normalized activity for each animal (Fig. 1, G and H). These data represent a population response to two different events: (i) the appearance of the target and the subsequent generation of the memory-guided saccade, and (ii) the appearance of the distractor. Although we recorded the response of each of the neurons to those two events, one could as easily reinterpret the activity as that simultaneously seen in two different populations of neurons, one with receptive fields at the saccade goal and the other with receptive fields at the distractor site.

A comparison of the monkeys' performance (Fig. 2, A and B, triangles) with activity in LIP (Fig. 2, A and B, lower plots) reveals a consistent relation between activity in LIP and the region of enhanced sensitivity. At any given time throughout the trial, the attentionally advantaged part of the visual field was that which lay in the receptive fields of LIP population with the highest discharge. There was no direct relationship between the absolute amount of activity at a given site in LIP and the attentional advantage. The attentional advantage appeared to be binary, whereas the activity in LIP was graded.

The appearance of the distractor outside of the receptive field had no significant effect on the delay period activity across the sample as a whole and in all but four cells (fig. S2A). As activity in the distractor population began to wane, there was a small but significant increase in the discharge rate of the target population (fig. S2B). Soon after, the level of activity evoked by the flashed distractor crossed the level of activity in the target population. For each monkey, there was a window of 80 to 90 ms (its time of equal activity or window of ambiguity) in which there was no significant difference between the activity evoked by the distractor and the activity related to the saccade plan ($P > 0.05$ by Wilcoxon signed-rank test, gray columns in Fig. 2, A and B).

After we determined the time of this window of ambiguity, we went back and measured the contrast thresholds at the saccade goal and at the distractor site at three different times for each monkey: its time of equal

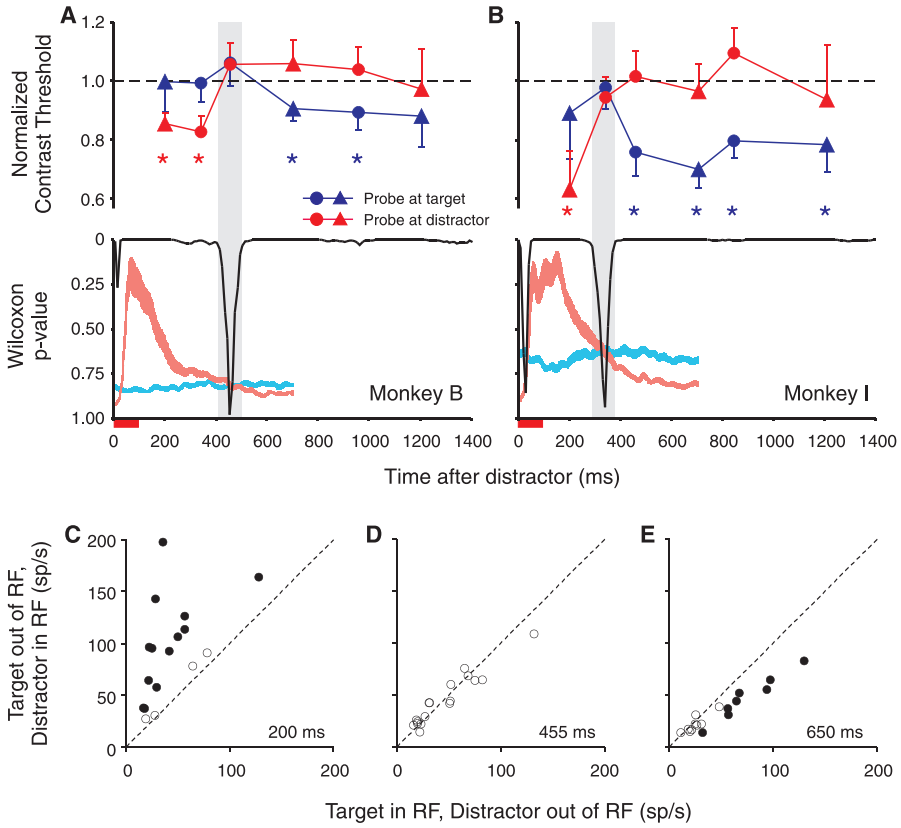

Fig. 2. Comparison of LIP response and monkey behavior. (**A** and **B**) Top: Behavioral performance of the monkeys when the probe was placed in the target (blue) or distractor (red) location in trials in which the target and distractor were in opposite locations. Triangles represent data shown in Fig. 1, C and D; circles represent data from psychophysical experiments performed after the single-unit data in Fig. 1, E to H, were recorded. Bottom: Black traces show the *P* values from Wilcoxon paired signed-rank tests performed on the activity of all the neurons for a monkey over a 100-ms bin, measured every 5 ms. Red and blue traces are taken from Fig. 1, G and H. The vertical gray column signifies the period when there is no statistical difference between the activity in both populations. In each monkey, there was no psychophysical attentional advantage when there was no significant difference in the neuronal response. (**C** to **E**) A comparison of the activity when the distractor, but not the target, was in the receptive field (RF) with the activity when the target, but not the distractor, was in the receptive field, from one monkey. These plots represent three of the time periods measured to make the black trace in (A). Solid circles represent cells with significant differences in response (*t* test, $P < 0.05$). Sp/s, spikes per second. (C) Mean activity 150 to 250 ms after the onset of the distractor for monkey B. (D) Mean activity during a 100-ms epoch centered at the point of equal activity for monkey B (455 ms after the onset of the distractor). (E) Mean activity 600 to 700 ms after the onset of the distractor for monkey B.

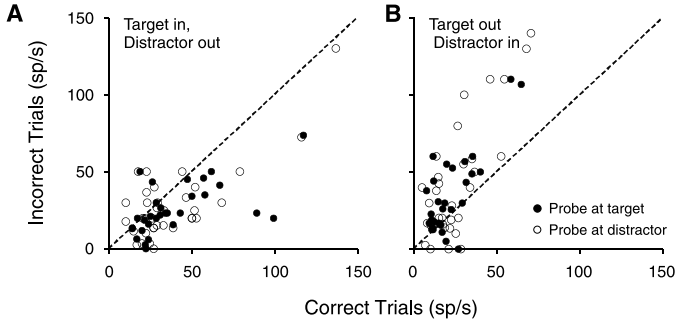

Fig. 3. Comparison of activity in correct and incorrect trials 100 ms before the appearance of the probe, plotted separately for probe location. (**A**) Trials in which the target, but not the distractor, appeared in the receptive field. (**B**) Trials in which the distractor, but not the target, appeared in the receptive field. Data are shown only for neurons that had errors in both stimulus configurations.

activity and 500 ms later (455 and 955 ms for monkey B and 340 and 840 ms for monkey I) and the other monkey's time of equal activity (Fig. 2, A and B, circles). At the time of equal activity, there was no spatial region of enhanced sensitivity in either monkey, but within 500 ms attention had shifted back to the site of the target in both monkeys, with normalized thresholds similar to those seen in the earlier experiment. Furthermore, each monkey had the appropriate attentional and neuronal advantages at the other monkey's time of neuronal ambiguity.

Although at times there is only a small difference in the normalized activity of neurons representing the attentionally advantaged and unadvantaged spatial locations, this difference is extraordinarily robust across the population (Fig. 2, C to E). We included all classes of neurons that we encountered, because the major outputs from LIP are produced by all the classes of neurons found in LIP (*27*, *28*), and we have separately illustrated those with (solid circles) and without (open circles) statistically significant differences in their responses ($P < 0.05$ by t test). Generally, those neurons without significant differences in late-delay activity (Fig. 2E) were those that had no activity during the delay period of the memory-guided saccade task.

There was also a relation between the performance of an animal and activity in its LIP during the 100 ms before the probe appeared in correct and incorrect trials for the two stimulus configurations (Fig. 3). The activity evoked by the saccade plan was lower on error trials than on correct trials, but the activity evoked by the distractor was higher on error trials than on correct trials. This activity did not vary with probe location.

Neuronal responses to the probe. Many previous studies have suggested that an enhanced parietal response to an object reflects attention to that object (*2*, *29*, *30*). We found instead that the responses evoked by the probe itself did not correlate with our measure of attention. When the probe was in the receptive field, the initial on-responses were identical whether the cue dictated GO to the receptive field, GO elsewhere, or NOGO (Fig. 4, A and B). After 100 ms, these responses diverged. When the probe signaled GO elsewhere, the response fell rapidly (blue trace). When the probe signaled GO to the receptive field, the response fell more slowly and returned to the pre-probe delay-period level (green trace). When the probe signaled NOGO and the monkey was planning a saccade to the receptive field, the response fell far less rapidly, as if a stimulus requiring a cancellation of the planned saccade evoked attention longer than one confirming it (red trace). Across the sample, the response to this cancellation was significantly greater than the response to the confirmation signal when the saccade plan was to the receptive field (Fig. 4C), and even more so when the saccade plan and its associated attentional advantage were directed away from the receptive field (Fig. 4D). When the response finally fell, however, it fell to the level of the GO-elsewhere response. We found no difference between the response to the GO probe (a Landolt ring) and the response to the complete rings in trials in which the saccade plan was directed to the receptive field (Fig. 4E) or away from it ($P > 0.2$, Wilcoxon paired signed-rank test). Nor was there any difference in the on-responses to the probe in correct and in-

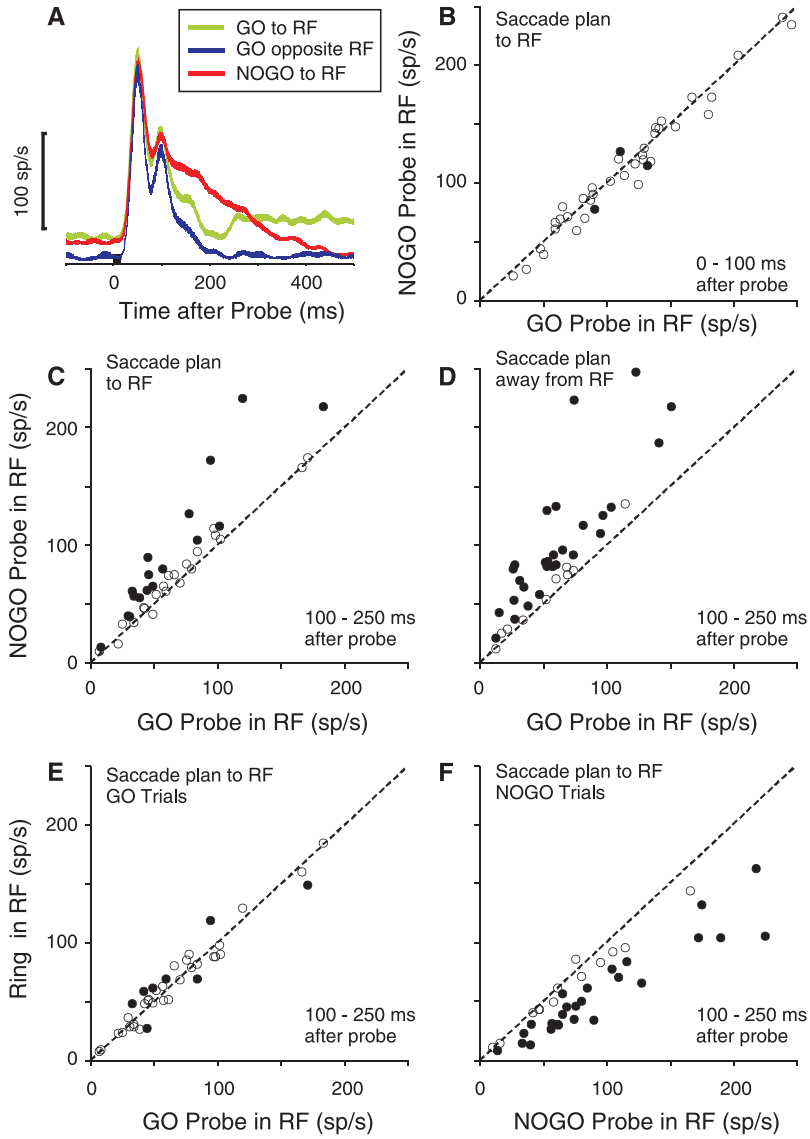

Fig. 4. The response to the probe in the receptive field. (**A**) Spike density functions from the same neuron illustrated in Fig. 1, E and F. Data are from trials in which the monkey was instructed to plan a saccade into the receptive field, and either the GO stimulus (green trace) or the NOGO stimulus (red trace) appeared in the receptive field, and from trials in which the saccade goal was opposite the receptive field and the GO probe appeared in the receptive field (blue trace). The timing of the stimulus presentation is represented by the black bar starting at 0 ms. (**B**) The response to the NOGO stimulus plotted against the response to the GO stimulus in trials in which the monkey was instructed to plan a saccade to the receptive field. In (B) to (F), solid circles show data from cells in which the difference in activity was significant ($P < 0.05$, t test); open circles show data from cells in which there was no significant difference. (**C**) The response to the NOGO stimulus plotted against the response to the GO stimulus in trials in which the monkey was instructed to plan a saccade to the receptive field. (**D**) The response to the NOGO stimulus plotted against the response to the GO stimulus in trials in which the monkey was instructed to plan a saccade away from the receptive field. (**E**) The response to the complete ring plotted against the response to the GO stimulus in trials in which the monkey was instructed to plan and execute a saccade to the receptive field. (**F**) The response to the complete ring plotted against the response to the NOGO stimulus in trials in which the monkey was instructed to plan and then cancel a saccade to the receptive field.

correct trials. However, the enhanced cancellation response was only seen for the actual NOGO probe and not for a ring in the receptive field when the NOGO probe appeared outside of the receptive field (Fig. 4F).

LIP and attention: A new perspective. Whenever we found an attentional advantage in performance, whether it was driven by the upcoming saccade or by the flashed distractor, the perceptual advantage at the attended location was always the same. However, the activity in LIP was graded. Thus, the attentional advantage lay in the spatial location subtended by the receptive fields of the neurons with the greatest activity, regardless of the absolute value of that activity. For instance, the activity at the saccade goal was sufficient to sustain the attentional advantage until it was swamped by the activity evoked by the distractor. Because of the fall of the visual transient evoked by the distractor, there was a period of about 90 ms, the window of neuronal ambiguity, during which the activity evoked by the saccade plan and distractor did not differ. Although the activity at both locations was above baseline, there was no attentional advantage at either site.

Thus one cannot ascertain a monkey's locus of attention by measuring the activity of a single neuron in LIP, or even by measuring the activity of all the neurons in whose receptive field a given object lies. Instead, one must look at the activity of the ensemble of LIP neurons representing all of the visual field. In this case, we can interpret the graded responses of the discharge at a given site in LIP as providing an attentional priority associated with the object in the subtended receptive field. We found little or no interaction within LIP, suggesting that the attentional priority of each part of the field is predominantly independent. Furthermore, evidence that attention encompasses a region of visual space around the attended stimulus has been found both psychophysically (*31*) and physiologically (*32*).

It is unclear what regions of the brain may be involved in the process we have suggested. Other cortical and subcortical areas show modulation of activity that may be related to the allocation of attention, such as the frontal eye field (*33*, *34*) and the superior colliculus (*35*). Indeed, microstimulation of the frontal eye field has been shown to improve performance in a contrast sensitivity task (*16*). However, the anatomical projections and graded responses seen in most of these areas suggest that they participate, along with LIP, in a distributed network that drives visual attention. We suggest that it is this distributed network that provides the bias for the biased competition model of attention postulated by Desimone and Duncan (*36*).

The visual activity of neurons in the posterior parietal cortex is modulated by the salience of the stimulus in their receptive fields (*4*, *29*). Such enhanced responses have been considered to reflect the attention to the object that evokes the response (*2*, *10*); however, a few studies have called this concept into question. For instance, the intensity of responses in the ventral intraparietal and middle temporal areas did not correlate with the attention paid to the stimuli (*30*); in a cued visual attention task, the activity evoked by a validly cued stimulus was less than that evoked by an invalidly cued one, even though attention lay at the site of the validly cued stimulus (*3*). It has been suggested that LIP is more important in determining a shift of visual attention to a stimulus than in maintaining attention to it (*3*, *37*). Our results show that the activity in LIP does, in fact, continuously describe the locus of attention but that this cannot be determined by looking at only one neuron or the representation in LIP of one spatial location. Although LIP does describe the locus of attention, the activity evoked by a stimulus does not necessarily define the attention to that stimulus. We postulate that the enhanced response evoked by an attended stimulus serves to reinforce the attentional priority of its locus rather than providing an original attentional selection.

The locus of attention is defined by a leftward shift in a psychophysical curve and not by performance on a trial-by-trial basis. However, activity in LIP did predict monkey behavior in one sense: When a monkey performed the task correctly, responses to the distractor measured in the 100 ms before the probe appeared were less than when the monkey failed to perform the task correctly, even on those trials in which the probe appeared at the distractor site. Conversely, activity at the saccade goal was greater on correct trials, even when the NOGO probe appeared at the saccade goal. We suggest that this activity in LIP provides a general index of the quality of a monkey's performance: When a monkey was doing its job efficiently, activity at the saccade goal was greater and the response to the distractor was weaker. Thus, the ratio of the activity at the saccade goal and at the distractor predicts the efficiency of a monkey's performance, regardless of the actual geometry of the task.

Attention and motor intention. A number of studies have suggested that LIP is a part of the system for planning saccadic eye movements, on the basis of its activity in the delayed saccade task (*38*–*43*). The strongest evidence for this is that delay-period activity of LIP neurons is greater when the neurons describe the target of a saccade than when they describe the target of a simultaneously generated arm movement to a different location (*38*–*39*). In light of our current findings, we would interpret these data as predicting that the saccade goal should have a higher attentional priority than the reach goal (*17*, *21*). Furthermore, our results render the motor intention interpretation unlikely for a number of reasons. The first is that visual attention is pinned to the spatial location of a saccade goal for the duration of the delay period in a memory-guided saccade task; therefore, one cannot distinguish a priori whether LIP activity during the delay period is related to attention or to a motor plan. The second is that when there is a separation between the locus of attention and the saccade goal, the ensemble of neurons in LIP accurately predicts the locus of attention even when there is a conflict between the motor plan and the current locus of attention. Conversely, LIP activity does not predict where, when, or even if a saccade will occur (*5*, *6*). Because attention is ordinarily pinned at the goal of a saccade, it is not unreasonable for LIP to have a faithful replica of a saccade plan. However, because of the many other attention-worthy events that also drive LIP, the saccade plan can be contaminated in a way that renders it useless as a motor signal. In fact, concurrent recordings of local field potentials (which represent synaptic input to LIP) and single-unit recordings have shown that the inputs to LIP contain far more information about an upcoming saccade than the spiking outputs do (*44*). The third and most dramatic reason is the activity in LIP evoked by the NOGO signal at the saccade goal. This activity is greater than that evoked by the GO signal at the same site. It is difficult to argue that a motor intention signal increases for several hundred ms in response to a signal canceling the intended movement and responds less to a signal confirming it. It is far easier to argue that one attends more to a signal requiring a change of plan than to a signal that confirms the plan.

Of course, LIP has a strong projection to the oculomotor system, with monosynaptic projections to and from the frontal eye field and monosynaptic projections to and disynaptic projections from the superior colliculus (*45*). Generally, there is a strong correlation between attended objects and saccade targets in the visual field (*18*, *46*). However, this correlation is not obligate, and our results show that in the very circumstances where there is dissonance between a saccade plan and LIP activity, the oculomotor system must ignore LIP. In contrast, we are unaware of any exception to the correlation between the ensemble of activity in LIP and the attentionally advantaged spatial location.

References and Notes

1. R. A. Rensink, *Vision Res.* **40**, 1469 (2000).
2. C. L. Colby, J. R. Duhamel, M. E. Goldberg, *J. Neurophysiol.* **76**, 2841 (1996).
3. D. L. Robinson, E. M. Bowman, C. Kertzman, *J. Neurophysiol.* **74**, 698 (1995).
4. J. P. Gottlieb, M. Kusunoki, M. E. Goldberg, *Nature* **391**, 481 (1998).
5. J. Gottlieb, M. E. Goldberg, *Nature Neurosci.* **2**, 906 (1999).

6. K. D. Powell, M. E. Goldberg, *J. Neurophysiol.* **84**, 301 (2000).
7. M. A. Steinmetz, C. E. Connor, C. Constantinidis, J. R. McLaughlin, *J. Neurophysiol.* **72**, 1020 (1994).
8. S. Yantis, J. Jonides, *J. Exp. Psychol. Hum. Percept. Perform.* **10**, 601 (1984).
9. H. E. Egeth, S. Yantis, *Annu. Rev. Psychol.* **48**, 269 (1997).
10. M. E. Goldberg, R. H. Wurtz, *J. Neurophysiol.* **35**, 560 (1972).
11. M. I. Posner, *Q. J. Exp. Psychol.* **32**, 3 (1980).
12. E. M. Bowman, V. J. Brown, C. Kertzman, U. Schwarz, D. L. Robinson, *J. Neurophysiol.* **70**, 431 (1993).
13. E. A. Witte, M. Villareal, R. T. Marrocco, *Behav. Brain Res.* **82**, 103 (1996).
14. H. S. Bashinski, V. R. Bacharach, *Percept. Psychophys.* **28**, 241 (1980).
15. V. M. Ciaramitaro, E. L. Cameron, P. W. Glimcher, *Vision Res.* **41**, 57 (2001).
16. T. Moore, M. Fallah, *Proc. Natl. Acad. Sci. U.S.A.* **98**, 1273 (2001).
17. E. Kowler, E. Anderson, B. Dosher, E. Blaser, *Vision Res.* **35**, 1897 (1995).
18. H. Deubel, W. X. Schneider, *Vision Res.* **36**, 1827 (1996).
19. Materials and methods are available as supporting material on *Science* Online.
20. M. Shepherd, J. M. Findlay, R. J. Hockey, *Q. J. Exp. Psychol. A* **38**, 475 (1986).
21. J. E. Hoffman, B. Subramaniam, *Percept. Psychophys.* **57**, 787 (1995).
22. The mean normalized thresholds (±SEM) for the three nontarget locations were 1.03 ± 0.05, 1.02 ± 0.06, and 0.95 ± 0.03 for monkey B and 1.01 ± 0.08, 1.04 ± 0.08, and 0.95 ± 0.06 for monkey I.
23. The mean asymptotic performances (±SEM) at and away from the saccade goal were 90.7 ± 1.2% and 90.0 ± 1.2% for monkey I and 94.2 ± 0.7% and 93.0 ± 0.7% for monkey B. The mean slopes (±SEM) at and away from the saccade goal were 2.37 ± 0.43 and 2.34 ± 0.32 for monkey I and 2.22 ± 0.34 and 2.59 ± 0.28 for monkey B.
24. K. Nakayama, M. Mackeben, *Vision Res.* **29**, 1631 (1989).
25. S. Yantis, J. Jonides, *J. Exp. Psychol. Hum. Percept. Perform.* **22**, 1505 (1996).
26. J. S. Joseph, L. M. Optican, *Percept. Psychophys.* **58**, 651 (1996).
27. M. Pare, R. H. Wurtz, *J. Neurophysiol.* **85**, 2545 (2001).
28. S. Ferraina, M. Pare, R. H. Wurtz, *J. Neurophysiol.* **87**, 845 (2002).
29. M. C. Bushnell, M. E. Goldberg, D. L. Robinson, *J. Neurophysiol.* **46**, 755 (1981).
30. E. P. Cook, J. H. Maunsell, *J. Neurosci.* **22**, 1994 (2002).
31. D. LaBerge, R. L. Carlson, J. K. Williams, B. G. Bunney, *J. Exp. Psychol. Hum. Percept. Perform.* **23**, 1380 (1997).
32. C. E. Connor, D. C. Preddie, J. L. Gallant, D. C. Van Essen, *J. Neurosci.* **17**, 3201 (1997).
33. A. Murthy, K. G. Thompson, J. D. Schall, *J. Neurophysiol.* **86**, 2634 (2001).
34. T. Sato, A. Murthy, K. G. Thompson, J. D. Schall, *Neuron* **30**, 583 (2001).
35. M. A. Basso, R. H. Wurtz, *J. Neurosci.* **18**, 7519 (1998).
36. R. Desimone, J. Duncan, *Annu. Rev. Neurosci.* **18**, 193 (1995).
37. S. Yantis *et al.*, *Nature Neurosci.* **5**, 995 (2002).
38. L. H. Snyder, A. P. Batista, R. A. Andersen, *Nature* **386**, 167 (1997).
39. L. H. Snyder, A. P. Batista, R. A. Andersen, *J. Neurophysiol.* **79**, 2814 (1998).
40. M. L. Platt, P. W. Glimcher, *J. Neurophysiol.* **78**, 157 (1997).
41. P. Mazzoni, R. M. Bracewell, S. Barash, R. A. Andersen, *J. Neurophysiol.* **76**, 1439 (1996).
42. R. M. Bracewell, P. Mazzoni, S. Barash, R. A. Andersen, *J. Neurophysiol.* **76**, 1457 (1996).
43. R. A. Andersen, C. A. Buneo, *Annu. Rev. Neurosci.* **25**, 189 (2002).
44. B. Pesaran, J. S. Pezaris, M. Sahani, P. P. Mitra, R. A. Andersen, *Nature Neurosci.* **5**, 805 (2002).
45. R. A. Andersen, C. Asanuma, G. Essick, R. M. Siegel, *J. Comp. Neurol.* **296**, 65 (1990).
46. A. L. Yarbus, *Eye Movements and Vision* (Plenum, New York, 1967).

47. We are grateful to the staff of the Laboratory of Sensorimotor Research for assistance in all aspects of this study: J. Raber and G. Tansey for veterinary care; N. Nichols and T. Ruffner for machining; J. McClurkin for help with graphics programming; L. Jensen for electronics; A. Hays for systems programming; C. Rishell and M. Szarowicz for animal care; R. Desimone for comments on a previous version of the manuscript; and M. Smith, J. Steinberg, and B. Harvey for facilitating everything. Supported by the National Eye Institute, the W. M. Keck Foundation, and the Human Frontiers Science Program.

Supporting Online Material

www.sciencemag.org/cgi/content/full/299/5603/81/DC1
Materials and Methods
Supporting Text
Figs. S1 and S2
References and Notes

15 August 2002; accepted 23 October 2002

REPORTS

Dependence of Upper Critical Field and Pairing Strength on Doping in Cuprates

Yayu Wang,[1] S. Ono,[2] Y. Onose,[3] G. Gu,[4] Yoichi Ando,[2] Y. Tokura,[3,5] S. Uchida,[6] N. P. Ong[1]*

We have determined the upper critical field H_{c2} as a function of hole concentration in bismuth-based cuprates by measuring the voltage induced by vortex flow in a driving temperature gradient (the Nernst effect), in magnetic fields up to 45 tesla. We found that H_{c2} decreased steeply as doping increased, in both single and bilayer cuprates. This relationship implies that the Cooper pairing potential displays a trend opposite to that of the superfluid density versus doping. The coherence length of the pairs ξ_0 closely tracks the gap measured by photoemission. We discuss implications for understanding the doping dependence of the critical temperature T_{c0}.

The superconducting state in a metal is completely suppressed if a sufficiently strong magnetic field is applied. In individual type-II superconductors, the field required—defined as the upper critical field H_{c2}—is an important parameter because it determines the value of the coherence length ξ_0 (the size of the Cooper pair) as well as the strength of the pairing potential; the higher the field H_{c2}, the stronger is the pairing potential and the smaller the pair size (*1*). In the phase diagram of the cuprates, superconductivity has been observed in the range of hole concentration $0.05 < x < 0.25$. Many parameters of the superconducting state, notably the superfluid density and superconducting gap, have been measured as a function of x. The conspicuous exception is H_{c2}, which is uncertain for reasons discussed below. Because even the basic trend of H_{c2} versus x is unknown, the crucial question of whether the pairing strength, as distinct from the superfluid density, increases or decreases with x remains unanswered. We report measurements of H_{c2} versus x in the Bi-based cuprates using the vortex-Nernst effect. In both single and bilayer systems, it was found that H_{c2} (and hence the pairing potential) steeply decreased as x increased. We show that ξ_0 is intimately related to the gap measured by angle-resolved photoemission spectroscopy (ARPES) (*2*) and results from scanning tunneling microscopy (STM) (*3*, *4*).

In the Nernst effect (*5*–*11*), vortices in the vortex liquid state are driven down an applied temperature gradient $-\nabla T \| x$. Their velocity v

[1]Department of Physics, Princeton University, Princeton, NJ 08544, USA. [2]Central Research Institute of Electric Power Industry, Komae, Tokyo 201–8511, Japan. [3]Spin Superstructure Project, Japan Science and Technology, Tsukuba 305–8562, Japan. [4]Physics Department, Brookhaven National Laboratory, Upton, NY 11973, USA. [5]Department of Applied Physics, [6]School of Frontier Sciences, University of Tokyo, Tokyo 113–8656, Japan.

*To whom correspondence should be addressed. E-mail: npo@princeton.edu

Materials and Methods

All experimental protocols were approved by the NEI Animal Care and Use Committee as complying with the guidelines established in the Public Health Service Guide for the Care and Use of Laboratory Animals. Two male rhesus monkeys (*Macaca mulatta*) had scleral search coils, head restraining devices and recording chambers implanted during sterile surgery under ketamine and isofluorane anaesthesia. Chambers were positioned using magnetic resonance images, and neurons were identified as being in LIP by their consistent visual, delay-period and saccade related responses in the memory guided saccade task (*S1,S 2*).

Behavioral Task

Behavioral control and data collection were done on computers using the REX system (*S3*). The task (Fig. S1) had two components: the monkeys had to plan a saccade to a remembered location and then had to discriminate a GO/NOGO stimulus which instructed them to proceed with the saccade or cancel it. We used the saccade plan to establish a locus of attention, in keeping with many studies in humans that have shown that before a saccade is made attention is allocated to the goal of that saccade (*S4-S7*), and we used the contrast sensitivity of the probe to measure that attention independently. We measured the animal's GO/NOGO discrimination performance at a number of contrasts and calculated the contrast threshold, which we defined as the contrast at which the animal could correctly discriminate the probe in 75% of the trials.

Visual stimuli were projected on a tangent screen with a refresh rate of 60 Hz, so all events were accurate to within 17 ms. The background luminance was 15 cd/m^2 and the contrasts of the fixation point, target and distractor were 55% (measured with a Tektronix J17 Photometer). The contrast of the rings was varied methodically so that an approximately equal

number of trials began with each contrast level. In most of the physiological sessions, the luminance of the rings was suprathreshold to facilitate the collection of data. In the psychophysical sessions done without recording, the target and distractor were 0.2º in diameter, the rings were 0.2º thick and 2.2º in diameter and the gap in the Landolt ring was 0.8º. In the physiological sessions, the objects were scaled up in size to account for the eccentricity of the receptive field. All objects apart from the fixation spot were at 10º eccentricity for the psychophysics and between 6º and 34º eccentricity for the recording studies, depending on the location of the receptive field. During fixation animals had to keep within a 4 degree window, and they had 500 ms after the disappearance of the fixation spot to make a saccade to a window around the saccade goal or to maintain fixation within a window in the center of the screen to receive a drop of water as a reward. If the animal's gaze stayed in the correct window for 500 ms then a spot appeared to reinforce the choice and to ensure that the animal did not drift out of the window in the remaining time. The windows were scaled in size to account for eccentricity, but rarely overlapped with each other. In cases in which the windows overlapped we confirmed by inspection of each trial that the animals were within the non-overlapped region when rewarded. Psychophysical sessions were made up of 1500-2000 trials in which the 4 possible saccade goals remained constant, although the 4 locations changed on a daily basis; activity from neurons was recorded for approximately 200-400 trials in which the probe appeared at a suprathreshold level as judged by the monkeys' performance. In 4 cases threshold psychophysics was also run while recording from the neuron. These sessions lasted between 800-1600 trials.

Data analytic methods

Both monkeys' behavioral performances varied from day to day, so in order to compare performance on different days we normalized the data on a daily basis to the monkey's

performance on trials in which there was no distractor and the probe was not at the location of the saccade goal (i.e. the threshold from the right-hand function in the example in Fig. 1a). Statistical significance was confirmed with a paired t-test on the pre-normalized data. In the physiology experiments, a spike-density function (*S8*) was calculated for each trial by convolving the spike train, sampled at 1 kHz, with a Gaussian of sigma 10 ms. Neuronal responses were illustrated as the average of this spike-density trace over the interval of interest, across all common correct trials. To create the population data, each spike density function was normalized by the mean activity over all the functions for that cell and an average was made from all the cells from each animal. Normalization was also done by taking the square root of the activity and dividing it by the mean of the square roots of the activity, and also by using the maximal firing rate as normalizing factor. Each method of normalization gave the same temporal pattern of activity and the same point of equal activity. We also summed the data and found no difference in the timing of the response. Neuronal responses were compared by calculating the firing rate over a 100 ms epoch from different trial types. For single cells a t-test was used to compare the data statistically, and a Wilcoxon paired sign rank test was used for population comparisons. All data analysis programs were written in Matlab (Mathworks Inc), using its curve-fitting and statistical capabilities.

Supporting Text

In 4 neurons we recorded the activity of LIP neurons while the animal performed the task with the suprathreshold stimuli and then again with the full range of contrasts to see if there was any difference in the activity of the neurons in a more demanding situation. We calculated the mean rates of activity over 3 epochs (those used in Figs. 2C-E) for the two primary stimulus configurations (target in receptive field, distractor out, and distractor in

receptive field, target out) both when the monkey was working with all contrasts and with only the suprathreshold contrast. We found that the activity was the same regardless of the difficulty level – the regression coefficient for a line fitted through the 24 points (4 neurons x 3 epochs x 2 stimulus configurations) was 1.04 with a shift of 1.34 sp/s (R^2 of 0.91).

Supporting Figures

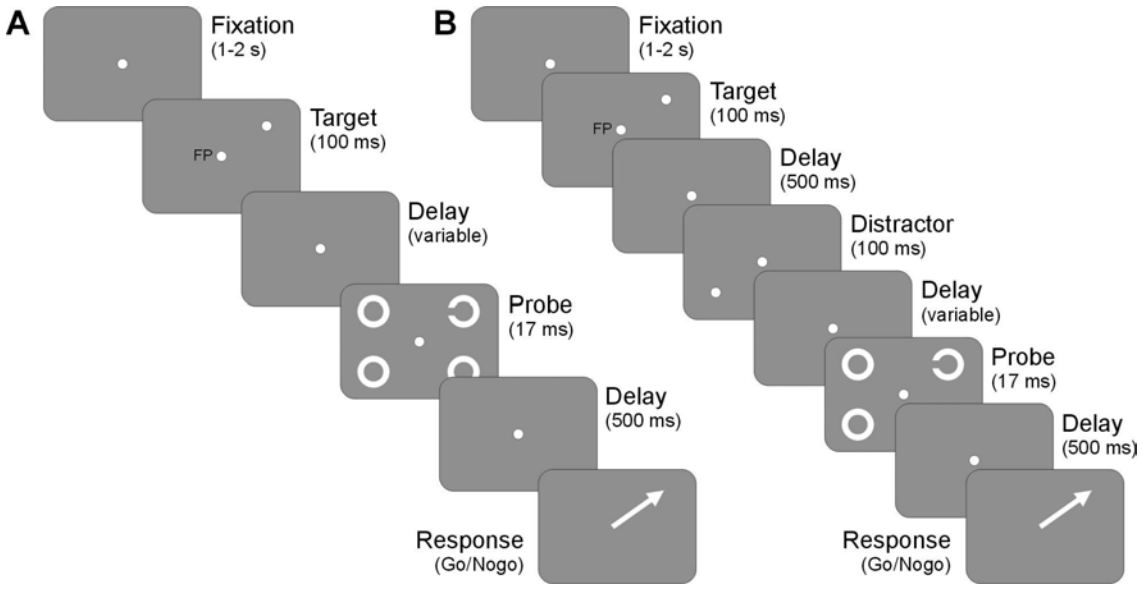

Figure S1. Psychophysical task. (**A**) The monkeys initiated a trial by fixating a small spot (FP) and after a short delay a second spot (the target) appeared for 100 ms at 1 of 4 possible positions equidistant from the fovea and evenly distributed throughout the 4 visual quadrants. The exact target locations varied from day to day, to prevent long-term perceptual learning, and also to render the monkey's behavior flexible enough so that target locations could be moved into the receptive field of any neuron that we studied. This target specified the goal for the memory-guided saccade that the monkey would have to make unless the probe told it

otherwise. At some time after the target disappeared, a Landolt ring (the probe) and three complete rings of identical luminance to the probe flashed for 1 video frame (~17ms) at the 4 possible saccade target positions. 500 ms after the probe the fixation point disappeared, and the animals had to indicate the orientation of the Landolt ring by either maintaining fixation for 1000 ms (when the gap was on the right – a NOGO trial) or making a saccade to the goal and remaining there for 1000 ms (when the gap was on the left – a GO trial). The Landolt ring could appear at any of the 4 positions. The luminance of the rings varied from trial to trial, changing the contrast between the probe and the background. (**B**) In half of the trials a task-irrelevant distractor, identical to the target, was flashed 500 ms after the target either at or opposite the saccade goal.

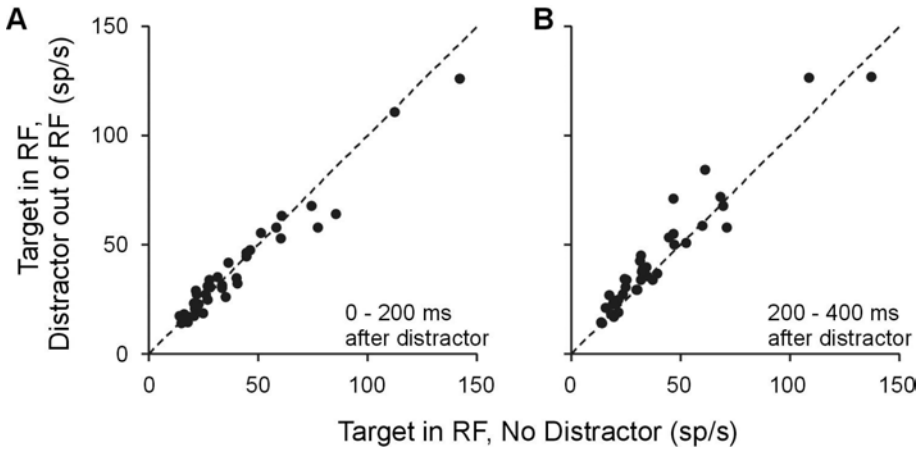

Figure S2. Effect of distractor appearance outside the receptive field on the delay response following the target. (**A**) Activity 0-200 ms after appearance of the distractor. The responses were not different across the population ($p > 0.4$, Wilcoxon paired sign rank test). (**B**) Response of same neurons 200-400 ms after distractor appearance. There was a small but significant difference in response across the population ($p < 0.002$).

Supporting References & Notes

S1. J. W. Gnadt, R. A. Andersen, *Exp. Brain Res.* **70**, 216 (1988).

S2. S. Barash, R. M. Bracewell, L. Fogassi, J. W. Gnadt, R. A. Andersen, *J. Neurophysiol.* **66**, 1095 (1991).

S3. A. V. Hays, B. J. Richmond, L. M. Optican, *WESCON Conf. Proc.* **2**, 1 (1982).

S4. M. Shepherd, J. M. Findlay, R. J. Hockey, *Q. J. Exp. Psychol.* **38**, 475 (1986).

S5. E. Kowler, E. Anderson, B. Dosher, E. Blaser, *Vision Res.* **35**, 1897 (1995).

S6. J. E. Hoffman, B. Subramaniam, *Percept. Psychophys.* **57**, 787 (1995).

S7. H. Deubel, W. X. Schneider, *Vision Res.* **36**, 1827 (1996).

S8. B. J. Richmond, L. M. Optican, M. Podell, H. Spitzer, *J. Neurophysiol.* **57**, 132 (1987).

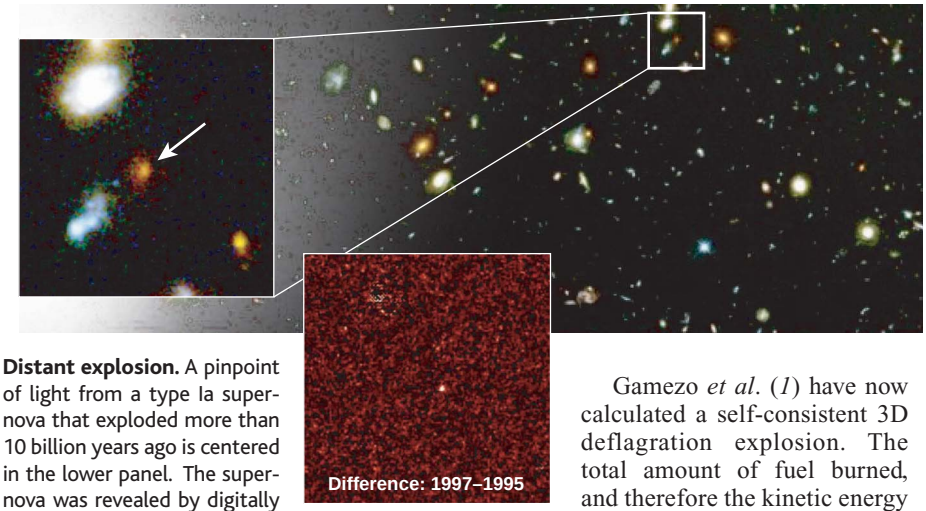

Distant explosion. A pinpoint of light from a type Ia supernova that exploded more than 10 billion years ago is centered in the lower panel. The supernova was revealed by digitally subtracting before and after images of a faint, yellowish, elliptical galaxy that appears in the Hubble Space Telescope Deep Field image shown at the top and left.

burning front is a subsonic nuclear flame. In a delayed detonation model, the deflagration makes a transition to a supersonic detonation. In both models, the velocity of the deflagration is crucial to the outcome, but it has to be treated as an adjustable parameter because the flame is inherently three-dimensional (3D). The density at which the deflagration-detonation transition (DDT) takes place also cannot be calculated in a 1D model.

Gamezo *et al*. (*1*) have now calculated a self-consistent 3D deflagration explosion. The total amount of fuel burned, and therefore the kinetic energy and the amount of ^{56}Ni, are about right to be consistent with observed light curves. The compositional structure, however, is quite unlike those of 1D models that are consistent with observation. Instead of being radially stratified, the elements coexist at all radii. The model spectra are unlikely to be consistent with observations.

The radially mixed compositional structure appears to be an inevitable characteristic of deflagration models, because buoyant burned matter such as ^{56}Ni and its decay products has time to rise relative to the denser unburned carbon and oxygen. Gamezo *et al*. (*1*) conclude that type Ia supernovae must undergo a DDT. Thus, by solving one problem they present another: Calculating DDT will be computationally challenging, especially considering the likelihood that DDT initiates almost simultaneously at various places in the ejected matter (*10*).

Now that 3D explosion models are beginning to appear, astronomers are gearing up to do 3D radiative transfer calculations so that the spectra of the models can be calculated and compared with observations (*11*–*12*). Supernova research is entering a new realm of computational complexity.

References and Notes

1. V. N. Gamezo, A. M. Khokhlov, E. S. Oran, A. Y. Chtchelkanova, R. O. Rosenberg, *Science* **299**, 77 (2003); published online 21 November 2002 (10.1126/science.1078129).
2. S. Perlmutter *et al*., *Astrophys. J.* **517**, 565 (1999).
3. A. G. Riess *et al*., *Astron. J.* **116**, 1009 (1998).
4. See http://snap.lbl.gov.
5. B. Leibundgut, *Annu. Rev. Astron. Astrophys.* **39**, 67 (2001).
6. K. Nomoto, K. Iwamoto, N. Kishimoto, *Science* **276**, 1378 (1997).
7. P. A. Mazzali *et al*., *Astron. Astrophys.* **269**, 423 (1993).
8. P. Ruiz-Lapuente *et al*., *Astrophys. J.* **439**, 60 (1995).
9. E. J. Lentz, E. Baron, D. Branch, P. H. Hauschildt, *Astrophys. J.* **557**, 266 (2001).
10. E. Livne, *Astrophys. J.* **527**, L97 (1999).
11. D. A. Howell, P. Hoflich, L. Wang, J. C. Wheeler, *Astrophys. J.* **556**, 302 (2001).
12. R. C. Thomas *et al*., *Astrophys. J.*, in press.

13. I thank M. Hamuy, R. Lopez, and A. Pastorello for providing the data for the first figure.

PERSPECTIVES: NEUROSCIENCE

To See Is to Attend

Steven Yantis

Neuroscientists who study vision are eager to discover how visual information is encoded in the pattern of neural activity within the more than three dozen visual areas of the brain. Complicating this task is the fact that vision is not a purely stimulus-driven, hard-wired response to visual input. The organism's state of attention, which depends on goals and expectations, strongly modulates visual responses in the brain (*1*–*4*). Indeed, it has been argued persuasively that we experience only that to which we attend (*5*). Attention is the means by which an organism controls the potentially overwhelming flow of visual input via top-down neural feedback. On page 81 of this issue, Bisley and Goldberg (*6*) provide new insights into how attentional control of vision is implemented in the primate brain.

Their study investigates neural activity in the lateral intraparietal area (LIP), a subregion of the parietal lobes (see the figure). The parietal cortex, in addition to analyzing visuospatial information and representing plans for limb and eye movements (*7*), also may be important for controlling the deployment of visual attention (*8, 9*). For example, responses in LIP and nearby parietal area 7a (see the figure) respond more strongly to stimuli that are salient or behaviorally relevant than to those that are not (*10, 11*). Functional neuroimaging studies have revealed selective activation of parietal areas during shifts of attention (*12*–*15*). However, no clear consensus has emerged about what neurons in the parietal cortex do.

To find out, Bisley and Goldberg trained two monkeys to perform a task that required them to prepare, but not immediately execute, a rapid eye movement or saccade. The monkeys had to plan a saccade from a central "home" location to a remembered location marked by a briefly flashed target dot (see the figure). They then had to decide whether to make the saccade on the basis of a subsequently flashed probe stimulus. If the probe was a "C" they were to make the saccade, but if it was a mirror-reversed "C" they were to withhold and cancel the saccade. Much previous work has shown that eye movements are preceded by a shift of attention to the new location (saccade goal) (*16*). In this monkey task, the maintained eye movement plan resulted in an increase in visual sensitivity at the saccade goal that was dependent on attention. The flashed probe could be accurately identified as a normal or mirror-reversed "C" at lower contrast when it appeared at the saccade goal, compared with when it appeared elsewhere. In this way, the monkey was induced to maintain a state of focused attention at the target location while waiting for the probe to appear.

Occasionally, a distractor dot was flashed in a nontarget location. This caused an involuntary, transient shift of attention to the distractor (*17*), indexed by increased perceptual sensitivity at the distractor location for a few hundred milliseconds after its appearance. The locus of attention then returned to the target location in preparation for the planned saccade. This task thus induced a sequence of

The author is in the Department of Psychological and Brain Sciences, Johns Hopkins University, Baltimore, MD 21218, USA. E-mail: yantis@jhu.edu

voluntary and involuntary attention shifts that occurred at well-specified times during the course of each trial of the experiment. Behaviorally, this was reflected in attention-dependent increases in perceptual sensitivity at the target, distractor, and target locations, in turn (see the figure). Bisley and Goldberg recorded the electrical activity of single neurons in the LIP area after mapping the cell's receptive field (the part of the scene that, when stimulated, drives the cell's response). They arranged the visual displays in the eye movement task so that either the target or the distractor dot would fall within the currently measured cell's receptive field.

When the target dot appeared, it evoked a strong transient neuronal response, followed by a sustained, above-baseline discharge that reflected the voluntary deployment of attention to the target location in preparation for the upcoming saccade (see the figure). When the distractor appeared elsewhere, it evoked a transient response in the population of LIP cells with receptive fields in the distractor location (and, importantly, this had no effect on the sustained discharge of the cell monitoring the target location). The response to the distractor returned to baseline within a few hundred milliseconds. Within the brief window of time during which the LIP cells monitoring the distractor location were most active, attention was fixed at that location. As soon as the LIP response in the distractor location fell below that in the target location, attention (as measured behaviorally) shifted back to the target location. For a very brief interval as the response to the distractor was decaying, and during which the responses of these two populations of cells did not differ, behavioral performance was similarly identical. This tight linkage between attention and the responses of LIP cells provides strong evidence that the LIP region of the parietal cortex constitutes a priority map of attention.

These findings offer a possible neural mechanism for an idea that has been advanced in the psychophysical and computational vision literature (*18–22*). According to these proposals, an attentional priority map continuously represents the importance or salience of every location in the visual field. Spatial attention is deployed to locations in the order of their priority; once visited, the priority at that location is canceled to prevent revisiting recently attended locations (called "inhibition of return") (*23*). Changes in the scene or in the observer's goals are dynamically reflected in the map.

A number of recent studies support a biased-competition model of visual selective attention, indicating a clear role for an attentional priority map (*1, 24, 25*). Populations of neurons tuned to specific sensory stimuli (for example, a red vertical bar versus a blue horizontal bar) compete for representation: When both stimuli are present in the scene, the response of each neural population is weaker than when either stimulus is presented alone. A top-down feedback signal that reflects the observer's state of attention is thought to bias the neural competition in favor of the attended object or location. This in turn reinforces the suppression of the unattended object. The attentional priority map may well be a source of the biasing signal.

Many questions remain to be answered. For example, Bisley and Goldberg induced attention shifts that were driven largely by the appearance of stimuli (although the maintenance of attention at the saccade goal required a voluntary intent). It would be of great interest to know whether these LIP cells behave in a similar way to shifts of attention that are purely top-down (for example, in response to an arbitrary auditory cue to attend to the upper right corner of the display).

Another open question is just how these parietal areas of the brain regulate sensory responses in extrastriate areas (for example, V4 and MT) that are known to be strongly modulated by attention (*3, 4, 15, 24, 25*). Bisley and Goldberg's observations, together with others that have implicated parietal activity in the control of voluntary shifts of attention (*2, 10–15*), suggest that parietal outputs may constitute the biasing signal for attention, but the causal link has not yet been definitively established.

Finally, little is known about how voluntary intentions give rise to changes in parietal and occipital areas. Prefrontal cortex—the site of working memory and executive control—is widely believed to be the ulti-

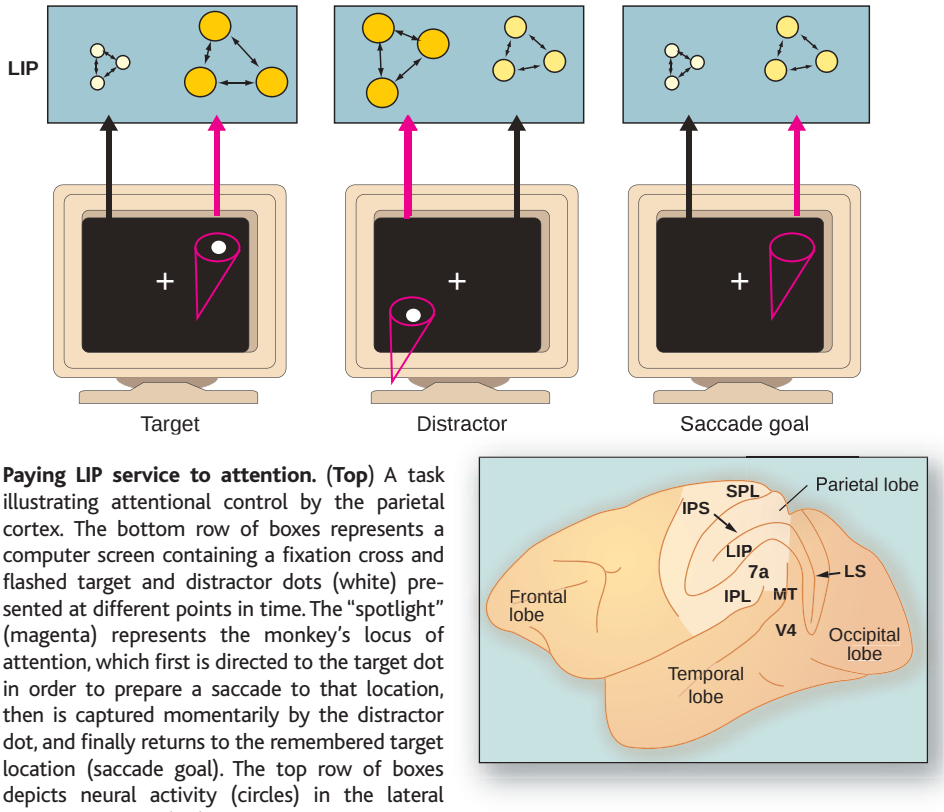

Paying LIP service to attention. (**Top**) A task illustrating attentional control by the parietal cortex. The bottom row of boxes represents a computer screen containing a fixation cross and flashed target and distractor dots (white) presented at different points in time. The "spotlight" (magenta) represents the monkey's locus of attention, which first is directed to the target dot in order to prepare a saccade to that location, then is captured momentarily by the distractor dot, and finally returns to the remembered target location (saccade goal). The top row of boxes depicts neural activity (circles) in the lateral intraparietal area (LIP) of the monkey brain. The white, yellow, and orange circles represent a low, medium, or high mean firing rate within a population of neurons. At the onset of the target dot (first column), there is a large transient burst of neural activity in LIP, followed by sustained activity that is lower than the peak but above baseline. This reflects the high attentional priority devoted to the location of the target dot (saccade goal). At the onset of the distractor dot (middle column), a large transient response, which dissipates rapidly, is evoked in LIP cells with receptive fields in that location. During the period of time that the distractor cells' response exceeds that of the target cells (after distractor onset), attention is pinned to the distractor location, yielding improved detection performance at this location. (**Bottom**) The brain of a macaque monkey showing the distinct subregions of the parietal lobes. These subregions mediate the planning of eye movements and visually guided limb movements, represent space, and control spatial and nonspatial attention. IPS, intraparietal sulcus; LS, lunate sulcus; SPL and IPL, superior and inferior parietal lobules; the IPS and LS are spread open to reveal the LIP, lateral intraparietal area; 7a, area 7a; V4 and MT, visual area 4, and middle temporal area, respectively.

CREDIT: KATHARINE SUTLIFF/*SCIENCE*

mate source of voluntary attentional control, but this is little more than speculation. Recent findings from monkey neurophysiology and functional brain imaging in humans are providing insights that will move us closer to answering these questions.

References

1. R. Desimone, J. Duncan, *Annu. Rev. Neurosci.* **18**, 193 (1995).
2. M. Corbetta, G. Shulman, *Nature Rev. Neurosci.* **3**, 201 (2002).
3. B. C. Motter, *J. Neurosci.* **14**, 2190 (1994).
4. K. M. O'Craven *et al.*, *Neuron* **18**, 591 (1997).
5. R. A. Rensink, *Vision Res.* **40**, 1469 (2000).
6. J. W. Bisley, M. E. Goldberg, *Science* **299**, 81 (2003).
7. L. H. Snyder *et al.*, *Nature* **386**, 167 (1997).
8. M. M. Mesulam, *Ann. Neurol.* **10**, 309 (1981).
9. S. Kastner, L. G. Ungerleider, *Annu. Rev. Neurosci.* **23**, 315 (2000).
10. J. P. Gottlieb *et al.*, *Nature* **391**, 481 (1998).
11. C. Constantinidis, M. A. Steinmetz, *Cereb. Cortex* **11**, 581 (2001).
12. M. Corbetta *et al.*, *J. Neurosci.* **13**, 1202 (1993).
13. E. Wojciulik, N. Kanwisher, *Neuron* **23**, 747 (1999).
14. R. Vandenberghe *et al.*, *Neuroimage* **14,** 661 (2001).
15. S. Yantis *et al.*, *Nature Neurosci.* **5**, 995 (2002).
16. J. E. Hoffman, B. Subramaniam, *Percept. Psychophys.* **57**, 787 (1995).
17. S. Yantis, J. Jonides, *J. Exp. Psychol. Hum. Percept. Perform.* **10**, 601 (1984).
18. C. Koch, S. Ullman, *Hum. Neurobiol.* **4**, 219 (1985).
19. B. A. Olshausen *et al.*, *J. Neurosci.* **13**, 4700 (1993).
20. J. M. Wolfe, *Psychon. Bull. Rev.* **1**, 202 (1994).
21. J. K. Tsotsos *et al. Artif. Intell.* **78**, 507 (1995).
22. D. Parkhurst *et al.*, *Vision Res.* **42**, 107 (2002).
23. R. M. Klein, *Trends Cogn. Sci.* **4**, 138 (2000).
24. S. Kastner *et al.*, *Science* **282**, 108 (1998).
25. J. H. Reynolds *et al.*, *J. Neurosci.* **19**, 1736 (1999).

Social Slime Molds Meet Their Match

Bernard Crespi and Stevan Springer

Alleles of genes that code for altruistic behavior face an identity crisis. Such behaviors are costly, and alleles that cause them can spread only if the benefits of altruism are preferentially directed to individuals that also carry the helpful allele. In most cases, altruistic individuals rise to this challenge probabilistically: They help relatives because their close genetic relationship makes them the best bet for carrying an identical allele. But even relatives are not a sure thing, and the cost of errant helping behavior could be avoided if alleles for altruistic behavior could directly recognize themselves in other individuals. Hamilton (*1*), in one of his legendary thought experiments, described three conditions that would allow a single gene to direct altruistic benefits toward a copy of itself in another individual. The three conditions are: (i) bearing a phenotype that advertises the allele's presence (such as a green beard), (ii) recognition of that phenotype in others, and (iii) an altruistic response (that is, preferential treatment) of those recognized. It was Dawkins (*2*) who coined the colorful metaphor "green beard" to denote such altruistic genes. Biologists had presumed that green-beard genes required too complex an integrated set of effects to have evolved. Their view changed, however, with the discovery of the fire ant gp9 locus (*3*) and the poison-antidote system of bacteriocin-producing bacteria (*4*). But these green-beard genes appear to comprise multiple tightly linked loci, so a single gene that could code for character, recognition, and response remained a theoretical curiosity. Enter Queller *et al*. (*5*) on page 105 of this issue with their description of single-gene green-beard effects in the slime mold *Dictyostelium*. Their work provides spectacular confirmation of Hamilton's musings and demonstrates that social behaviors thought too genetically complex even for altruistic metazoans like ourselves are present in the humblest eukaryotes ever to locomote over damp dirt.

Queller *et al*.'s finding that social behavior in *Dictyostelium* is facilitated by green-beard effects has been a long time coming but, as it turns out, is not entirely unexpected. In a feat of inductive logic as remarkable as Hamilton's initial proposal, Haig (*6*) described the potential for green-beard genes in maternal-fetal interactions. He even predicted the functional class of protein—a homophilic adhesion protein that binds to itself—that would ultimately yield the first single-gene green beard. Homophilic cell adhesion proteins have exactly the properties required to operate as single-gene green beards. These proteins display themselves conspicuously on the cell surface and function as simple self-recognition systems, that is, they bind to copies of themselves expressed by other cells. Altruistic benefits to other cells can result directly via benefits from aggregation or movement, or indirectly through intimate connections between cell adhesion proteins and intracellular signaling processes (*7*).

How does simple "find and bind" activity generate multifaceted social effects in slime molds? *Dictyostelium* exhibits altruistic behavior in its simplest and most extreme form. Starving single cells coalesce into a mass, which transforms into a fruiting body composed of two parts: reproductive spores and nonreproductive stalk cells that altruistically lift the spores high to aid their dispersal to a more food-rich environment (see the figure). Queller *et al*. recreated in the laboratory an evolutionary struggle for sporulation. They did this by pitting wild-type cells with a functional *csA* (contact site A) gene, encoding homophilic cell adhesion protein gp80, against knockout cells deficient in *csA* that showed defective adhesion. Their experiments revealed that wild-type, green-beard cells recognized and pulled one another into and along cooperative streams to the forming aggregate (mobile slug) via binding interactions among the homophilic cell adhesion proteins; but "clean-shaven" knockout cells were left far behind (see the figure). And with good reason—if knockout cells reached the aggregate, their reduced adhesion would displace them toward the trailing edge of the slug, an area that preferentially develops into spores. This would cause the good, green-beard cells to finish last. Such cheating is apparently disfavored, and green-beard alleles resist displacement by less adhesive mutants, just as green beards must have originally spread to supplant them. But might mutations also occur in beard genes encoding other colors, leading to clone-specific and thus nepotistic (rather than promiscuous) cooperation?

The discovery of molecular green beards has implications well beyond the niceties of slime mold social behavior. Single-gene green-beard effects could plausibly alter any biological process involving a close interaction between cells. Homophilic cell adhesion proteins were first studied because of their role in tissue differentiation. Tissue dedifferentiation leading to cancer is associated with expression of an altered suite of cell adhesion proteins, and metastasis correlates with reduced expression of this suite (*8*). Adhesion proteins whose expression is altered during tumor formation are all ideal green-beard candidates in a naturally selected although pathological context. Interactions between gametes can also be modified by green-beard effects. Cooperative sperm behavior, such as that of paired marsupial sperm (*9*) or wood mouse

The authors are in the Behavioural Ecology Research Group, Department of Biosciences, Simon Fraser University, Burnaby, BC V5A 1S6, Canada. E-mail: crespi@sfu.ca